Neural Network, Isotherm, and Kinetic Study for Wastewater Treatment Using *Populus alba's* Pruned Material

Pezhhanfar, Sakha
Department of Analytical Chemistry, Faculty of Chemistry, University of Tabriz, Tabriz, I.R. IRAN

Zarei, Mahmoud*[+]; Shekaari Teymourloue, Tohid
Research Laboratory of Environmental Remediation, Department of Applied Chemistry, Faculty of Chemistry, University of Tabriz, Tabriz, I.R. IRAN

Khalilzadeh, Mahdi
Department of Chemical & Petroleum Engineering, University of Tabriz, Tabriz, I.R. IRAN

ABSTRACT: *Dyes are utilized in several plants and factories. Contaminated wastewaters containing dyes cause many illnesses and have many adverse effects on humans, animals, and plants. This research aims to the usage of Populus alba tree's sawdust as a costless pruned agricultural waste material for the removal of crystal violet from simulated wastewater in batch adsorption experiments. The dye removal process by the adsorbent was performed by varying various parameters such as the weight of the adsorbent, pH of the solution, adsorption time, and the initial dye concentration. Generally, increasing the weight of the adsorbent and decreasing the initial dye concentration led to increasing removal efficiency. The optimum solution pH was found to be 6.5. Also, the optimum weight of the adsorbent and the optimum initial dye concentration were found to be 0.15 g and 10 mg/L, respectively. Moreover, the adequate adsorption time for the accomplishment of the treatment procedure was 10 min. Adsorption data were fitted well by the Langmuir adsorption isotherm model and the maximum amount of the adsorbate on the adsorbent (q_{max}) was calculated to be 12.25 mg/g. The kinetic study data illustrated the adaption of the adsorption rate with the pseudo-second-order kinetic model. The results of the ANN model proved the fitness of theoretical and experimental data according to the obtained correlation coefficient values. Eventually, the dye removal efficiency reached 97% in the optimum conditions of the experiments. So the sawdust of Populus alba tree's pruned hardwood is introduced as a costless and highly capable adsorbent for the adsorption of crystal violet from contaminated wastewaters in order to perform a successful wastewater treatment beside the accomplishment of a waste management procedure.*

KEYWORDS: *Populus alba tree; Wastewater treatment; Crystal violet; Isotherm study; Kinetic study; Artificial neural network.*

***** *To whom correspondence should be addressed.*
+ E-mail: zarei90211@yahoo.com & mzarei@tabrizu.ac.ir
1021-9986/2021/6/1868-1881 14/$/6.04

INTRODUCTION

Effluents of various industries such as textile, leather, cosmetics, food, dye manufacturing, and paper are contaminated with different dyes that are used for coloring aims [1, 2]. It is noteworthy to mention that about 10–15% of dyes used in textile industries are discharged through their sewages [3]. Mixing these polluted wastewaters with rivers and lakes not only contaminates them and affects their aesthetic appeal but also prevents sunlight penetration and reduces photosynthesis [4]. The presence of dyes in water bodies can be a predisposition for forming chelates with metal ions and they act as micro toxicity agents to endanger fish and the whole aquatic life [5]. Also, dyes can bring about skin irritation, dermatitis, and allergy, and result in cancer and mutation in humans [6]. Due to the fact that dyes have complex aromatic structures, they are mostly very resistant and stable against photo–degradation, bio–degradation, and oxidation processes [7]. Thus, the removal of dyes from contaminated effluents, particularly from textile industries, is one of the major environmental issues [8, 9]. Various methods such as foam flotation [10], coagulation [11], aerobic and anaerobic treatment [12, 13], filtration [14], ion exchange [15], solvent extraction [16], advanced oxidation processes [17], microbial reduction [18], adsorption [19], electrolysis [20], and sludge [21] are common for treatment of wastewater. Although the mentioned methods benefit from different aspects such as effective decolorization process but being laborious, time–consuming, costly, needing special and expensive instrumentations, and sludge and byproduct generation are the main drawbacks of some of the above–mentioned methods [22].

Among different wastewater remediation procedures, adsorption is of great importance. Transferring the dye molecules from the contaminated wastewater to a solid phase is the goal of this procedure [23]. Subsequently, the adsorbent can be reused for other purposes, regenerated, burnt for producing energy, or stored in a dry place for further applications according to its type and material. For example, activated carbon is a well–known and widely used adsorbent for the treatment of textile wastewaters due to its beneficial porous structure and having a high surface area. But because of being expensive, its utilization on a great scale has been limited [24]. Moreover, its adsorptive capability depends on both the type of organic substance applied for the manufacturing of activated carbon and the experimental conditions applied for the activation procedures [25]. Alum coagulation is another beneficial treatment process but it is not effective for the treatment of wastewaters containing acidic, basic, azoic, and reactive dyes [26]. Among various types of adsorbents, economic adsorbents are of great importance now. Natural adsorbents especially agricultural waste materials are so beneficial in wastewater treatment procedures due to many reasons such as simplicity in experimental design, performance in atmospheric pressure and room temperature, being free, widespread, abundant in nature, easily accessible, highly effective, environmentally friendly, having a simple application, and no byproducts [27, 28]. Different materials such as hardwood sawdust [29], *peanut* hull [30], Iranian *Sesamum Indicum* hull [9], Indian *rosewood* sawdust [31], *parthenium hysterophorus* [32], *cotton* plant wastes [33], *neem* sawdust [28], *orange* peel [34], *tea* waste [19], and pretreated *Sesamum* waste [35] have been used in many wastewater treatment processes.

Populus alba is a prevalently planted tree from central Europe to central Asia. It grows in humid places with cold to mild winters and hot summers. It grows up to 16–27 m. *Populus alba* belongs to the clade *Angiosperms*, order *Malpighiales*, family *Salicaceae*, and genus *Populus* [36]. Due to the fact that *Populus alba* is also an ornamental tree, pruning its old, broken, and deadwood branches is performed regularly. Moreover, since *Populus* wood is widely used for carpentry and woodcraft production purposes, pruning can be a helpful way to increase its growth rate. So, the sawdust of the deadwood parts obtained from the pruning procedure is mostly useless and can be utilized as an efficient adsorbent in the treatment procedure of contaminated wastewaters with dyes besides the accomplishment of a waste management process. Consequently, this colored sawdust can be used for the production of particleboards with veneer.

According to the importance of wastewater treatment from synthetic dyes prior to discharging in downstream water bodies the present research was accomplished. The main aim of the present research study is to develop a highly efficient, inexpensive, freely available and abundant, environmentally friendly, and byproduct-free adsorbent by using an agricultural waste material (sawdust of *Populus alba* tree's pruned hardwood) in order to fulfill a successful wastewater treatment procedure (the removal

of crystal violet from simulated wastewater) based on adsorption process and moreover, the potential utilization of the used and colored adsorbent in the process of *waste management* and production of wood-based materials such as particleboards with veneer, etc.

Through the experimental section fulfillment, the capability of the studied sawdust as a costless pruned agricultural waste material for the removal of crystal violet in batch adsorption experiments was established by varying various influencing parameters such as weight of adsorbent, pH of the solution, initial dye concentration, and adsorption time. Some isotherm models were investigated in the present wastewater treatment survey due to their importance for providing information around the capacity of the adsorbent or the amount required to remove a unit mass of pollutant under the system conditions. Moreover, some kinetic models were investigated to know the rate of the adsorption for the design and evaluation of the adsorption process. An Artificial Neural Network (ANN) was also designed and evaluated for the prediction of the wastewater treatment efficiency and to propose a suitable topology as like as input variables, number of neurons, and training algorithm. Additionally, FT-IR analysis was carried out to obtain comprehensive information about the adsorbent before and after the treatment procedure.

EXPERIMENTAL SECTION

Preparation of the adsorbent and the adsorbate

Waste parts of a *Populus alba* tree (locally called *Tabrizi tree*) were pruned and powdered by using a proper carpentry saw and the obtained powder was passed through a sieve (mesh No. 20). Then the adsorbent was put in a glass container at room temperature for further uses without any modifications.

The dye, crystal violet, with the molecular formula and mass of $C_{25}H_{30}ClN_3$ and 407.99 g/mol, respectively, was purchased from Sigma–Aldrich as the adsorbate in this research. Crystal violet is also known as gentian violet and its IUPAC name is Tris (4– (dimethyl amino) phenyl) methylium chloride. Potassium bromide, Sodium hydroxide, and hydrochloric acid (37%, *w/w*) were also supplied from Merck (all were of analytical grade). In the first step, a stock solution of the dye (1000 mg/L) was prepared by adding the proper amount of the dye powder in a 250 mL volumetric flask containing distilled water. Consequently, this solution was utilized for preparing other used solutions with different dye concentrations by diluting with distilled water.

Batch adsorption experiments

According to the UV–Vis spectra obtained by UV–Vis spectrophotometer (Analytik Jena, Specord 250, Germany) the maximum absorbance wavelength of the dye, λ_{max}, was found to be 591 nm. The analysis was fulfilled in a 400 mL glass beaker containing 100 mL dye solution with different dye concentrations (1, 3, 5, 7, 10, 15, 20, 25, 30, and 40 mg/L). Also various weights of the adsorbent were utilized in the treatment procedure (0.01, 0.03, 0.05, 0.07, 0.10, 0.13, 0.15, and 0.20 g). The effect of pH on the treatment process was investigated by adjusting the solution pH to the values of 2.5, 4.5, 6.5, 8.5, and 10.5. The desired solution pHs were modified using 0.1 mol/L NaOH and HCl by using a pH meter (Metrohm, 827, pH lab). The effect of adsorption time was evaluated in the range of 0–45 min. The batch system was located on a magnetic stirrer (Hotplate & Stirrer, JENWAY 1000, UK) by fixing the stirring rate at 300 rpm. During the treatment process, the samples were taken at regular time intervals and were poured into proper test tubes and put in a test tube rack, respectively. After the accomplishment of the adsorption processes, the taken solutions were centrifuged at 4000 rpm for 3 minutes using a centrifuge (Select–a–Fuge 24 BIO–DYNAMICS, USA) in order to perform the complete separation of the adsorbent particles from the treated solution. All the performed analyses were done at room temperature and atmospheric pressure. Fig. 1 illustrates the image of the adsorbent before (a) and after (b) the performance of the dye treatment procedure. Removal efficiency (RE) of the dye from the aqueous solution was computed as the percentage ratio of the adsorbed dye concentration to that of the initial dye concentration in the solution as shown in Eq. (1), in which C_i and C_f are the initial and final concentrations (mg/L) of the studied dye solutions, respectively.

$$RE\% = \frac{C_i - C_f}{C_i} \times 100 \quad (1)$$

FT-IR analysis

Fourier Transform InfraRed (FT-IR) technique is an exclusive method for the analysis of a material's functional

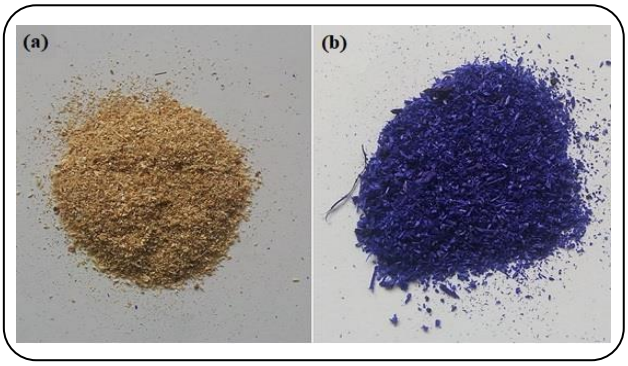

Fig. 1 Image of the adsorbent before (a) and after (b) the adsorption of crystal violet

groups. FT-IR analysis not only helps to characterize a chemical by the obtained exclusive spectra but also it helps to investigate and clarify the modifications and the probable changes in the studied material. The FT-IR instrumentation model (Tensor 27, Bruker, Germany) was utilized in this study to obtain the spectra of the adsorbent. So the properties of the studied adsorbent were investigated by FT-IR analysis before and after the dye loading procedure. For this purpose, a very little pinch of the adsorbent before and after the treatment were separately utilized to prepare FT-IR pellets by using KBr as the pellet bed. After mixing the adsorbent and KBr for 2 min, it was put under the press. Then the pellets were formed and subsequently analyzed by the FT-IR apparatus in the range of 400–4000 cm^{-1}. This process helps us to diagnose the functional groups of the applied adsorbent and the dye as the pollutant in order to prove the adsorption of dye on the adsorbent and also to obtain valuable information around the probable intramolecular interactions and mechanism of the adsorption.

Isotherm study of the adsorption procedure

The adsorption isotherms indicate how the studied molecules are distributed between the liquid and solid phases when the adsorption process reaches an equilibrium state. Langmuir, Freundlich, and Temkin, isotherm models were investigated in order to obtain comprehensive information about the adsorption procedure [37]. Langmuir isotherm model illustrates a monolayer adsorption procedure of an adsorbate on the limited sites of the adsorbent. For better saying, the Langmuir isotherm model is based on the assumption that there is a finite number of active sites which are homogeneously distributed over the surface of the adsorbent. These active sites have the same affinity for adsorption of a mono molecular layer and there is no interaction between the adsorbed molecules [38]. The Langmuir isotherm model's linear form is shown as Eq. (2).

$$\frac{C_e}{q_e} = \frac{1}{q_{max}} C_e + \frac{1}{b\, q_{max}} \quad (2)$$

In Eq. 2, the parameters q_e, C_e, b and q_{max} are the symbols for the weight of the pollutant adsorbed on the adsorbent at equilibrium, the equilibrium concentration of adsorbate, the constant of Langmuir isotherm, and the maximum monolayer coverage capacity, respectively. The variations of C_e / q_e *versus* C_e were drawn and the related parameters were calculated from the obtained line.

Freundlich isotherm is another helpful model which represents the heterogeneous surface of the adsorbent. This model is applied to the adsorption procedures on heterogeneous surfaces with interactions between the adsorbed molecules, and is not restricted to the formation of a monolayer. This model assumes that as the adsorbate concentration increases, the concentration of the adsorbate on the adsorbent surface also enhances, and correspondingly, the sorption energy exponentially decreases on completion of the sorption centers of the adsorbent [38]. The linear form of the Freundlich isotherm model is shown as Eq. (3).

$$\ln q_e = \ln k_f + \frac{1}{n} \ln C_e \quad (3)$$

The data C_e and q_e are described previously. In this model, the adsorption capacity is indicated as K_f, and $\frac{1}{n}$ illustrates the adsorption power in the process. The plot $\ln q_e$ *versus* $\ln C_e$ was drawn and the related data were computed using the acquired line.

Temkin and *Pyzhev* considered the effects of indirect adsorbate/adsorbate interactions on adsorption isotherms. The heat of adsorption of all the molecules in the layer would decrease linearly with coverage due to adsorbate/adsorbate interactions. Totally, Temkin isotherm model demonstrates that the coverage resulted from the adsorption of an adsorbate on the adsorbent results in dwindling the adsorption heat of molecules [9, 35]. The linear equation of the Temkin isotherm model is demonstrated as Eq. (40).

$$q_e = B \ln k_T + B \ln C_e \quad (4)$$

In this equation, B and k_T show the constants related to the heat of sorption and the isotherm equilibrium binding, respectively. The plot q_e *versus* ln C_e was drawn and the related values were calculated from the obtained line.

Adsorption kinetics study

Adsorption is a time-dependent procedure so the kinetic study is of great importance in the evaluation of an adsorption process to examine the controlling mechanism of dye adsorption from an aqueous solution by clarifying some prominent data such as adsorption rate, equilibrium time, and adsorption capacity [37]. Among various proposed kinetic models for the investigation of an adsorption process, the three; Weber–Morris intra–particle diffusion model and pseudo-first order and pseudo second-order models are prevalent. These three models basically include all steps of the adsorption such as external film diffusion, adsorption, and intra-particle diffusion, so they are called pseudo-models. The highest correlation coefficient (R^2) value obtained from the investigation of the linear forms of the kinetic models indicates the adherence of the adsorption procedure to that model [39, 40].

The pseudo-first-order model, known as the Lagergren's first-order rate equation which is the earliest known to describe the adsorption rate based on adsorption capacity, is generally being utilized in order to describe the rate of interactions between a solid and a liquid phase. This model illustrates that the occupation rate of the active sites is proportional to the number of active sites. It is worthwhile to mention that in some cases where rapid adsorption procedures occur, the first-order equation of Lagergren does not fit well for the whole range of contact time and is generally applicable over the initial 20-30 min of the sorption process. The linear form of the pseudo-first-order model is shown in Eq. (5).

$$\log\left(q_e - q_t\right) = \log q_e - \frac{k_1}{2.303} \times t \quad (5)$$

Where, k_1, q_e, and q_t stand for the rate constant of first-order adsorption procedure (min^{-1}), the adsorbed weight of the pollutant on the adsorbent (mg/g) at equilibrium, and adsorbed amount of the adsorbate on the adsorbent (mg/g) at any time of the adsorption procedure, respectively.

The pseudo second-order model is also an illustrative kinetic model for the evaluation of the rate of adsorption. This model assumes that the occupation rate of the active sites of the adsorbent with the adsorbate is proportional to the square number of the active sites on the adsorbent. The pseudo-second-order kinetic model is also based on the sorption capacity of the solid phase and on the assumption that the sorption process involves a chemisorption mechanism. Contrary to the first-order model it predicts the behavior over the whole range of contact time of the adsorption [41]. The linear form of the pseudo-second-order model is shown in Eq. (6).

$$\frac{t}{q_t} = \frac{1}{k_2 q_e^2} + \frac{1}{q_e} \times t \quad (6)$$

Where, k_2 is the rate constant of second-order adsorption procedure (min^{-1}), and q_e, and q_t are the previously mentioned parameter.

Weber–Morris model is based on diffusion which evaluates that the adsorbate transition from a liquid to a solid phase is based on film diffusion or pore diffusion. This kinetic model is totally based on the assumption that one or more than one adsorption process occurs in the experiment. In this model the intra–particle diffusion is considered as a rate–limiting step. The plot of this model may contain multi–linear parts, indicating that more than one step has occurred in the adsorption process. The first portion which is usually sharper is attributed to the diffusion of adsorbate through the solution to the external surface of the adsorbent or the boundary layer diffusion of the solute molecules. The second portion illustrates the slow and gradual adsorption stage, where intra–particle diffusion rate is rate–limiting. The probable third portion demonstrates the final equilibrium stage for which the intra–particle diffusion starts to slow down because of the low adsorbate concentration left in the solution. The adsorption rate can be limited by the size of the adsorbate molecule, the concentration of the adsorbate in the solution, the affinity of the adsorbate to the adsorbent, the diffusion coefficient of the adsorbate in the bulk phase, distribution of the pore size of the adsorbent, and degree of mixing. [42, 43]. The linear form of the Weber–Morris model is shown in Eq. (7).

$$q_t = k_i \times t^{1/t} + c \quad (7)$$

Where, k_i and c stand for intra–particle diffusion rate constant (mg g^{-1} $min^{-1/2}$), and intra–particle diffusion constant declaring the thickness of the boundary layer, respectively. Q_t is the previously mentioned parameter.

ANN Modeling

ANN, inspired by the structural and functional aspects of biological neural network, has attracted increasing attention in recent years, particularly for process modeling [44, 45]. It is now used as a very powerful tool to predict the behavior of a given system, to design new processes and analyze existing procedures [46, 47]. In designing an ANN model, predetermined inputs that are called independent variables reach a neuron and are carried forward by selected activation functions for the production of the output responses which are called dependent variables [48, 49]. The calculation process was accomplished using Matlab 2013 containing an ANN toolbox for the prediction of the wastewater treatment efficiency and to propose a suitable topology as like as input variables, number of neurons, and training algorithm [19, 35]. The designed algorithm was comprised of three layers with a sigmoidal transfer function (5:10:1) having a backpropagation. Input parameters were included as the adsorption time (0–45 min), adsorbent weight (0.01–0.2 g), pH of the solution (2.5–10.5), and the dye concentration (1–40 mg/L). The output parameter was the RE of the pollutant. The total data were 198 points that 60% of the data were devoted to training, 20% for validation, and 20% for the performed test series.

RESULTS AND DISCUSSION

Investigation of the effect of adsorbent weight

In order to evaluate the effect of the adsorbent weight on the RE of crystal violet from the aqueous solution, different weights of the adsorbent (0.01, 0.03, 0.05, 0.07, 0.10, 0.13, 0.15, and 0.20 g) were added in dye solutions with the concentration of 5 mg/L, 45 min adsorption time, and pH=6.5. Fig. 2 illustrates that 0.15 g of the adsorbent was the optimum weight and increasing the adsorbent amount more than that did not increase the REs. It is also worthwhile to mention that in lower weights of the applied adsorbent, the RE of the experiments dwindled because of decreasing the adsorptive surface area of the adsorbent. Therefore 0.15 g was chosen to be applied in further treatment experiments. Due to the fact that the adsorbent is a natural material, its repeatability of it was examined to make sure that the adsorbent performance is repeatable. So the optimum amount of the adsorbent (0.15 g) was chosen and the above-mentioned treatment experiment was repeated four times. The results illustrated that the REs% were so close that the RSD% was obtained to be 4.8%. Then the upcoming experiments were fulfilled conveniently being sure that the results of the wastewater treatment by using the present adsorbent has high repeatability.

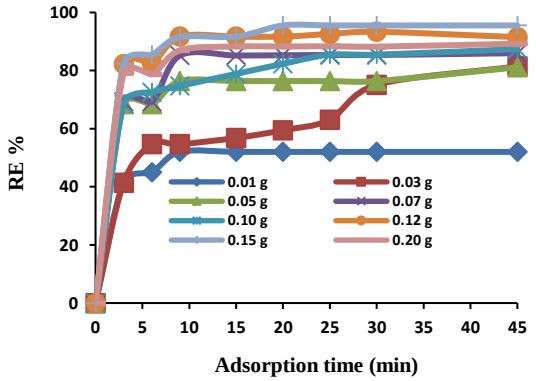

Fig. 2: Effect of the adsorbent weight on RE%. The concentration of the dye, 5 mg/L; pH=6.5; and adsorption time, 0–45 min.

Investigation of the effect of initial dye concentration

In order to ascertain the influence of the initial dye concentration on wastewater treatment efficiency, various concentrations of crystal violet (1, 3, 5, 7, 10, 15, 20, 25, 30, and 40 mg/L) were prepared by diluting the stock solution and 0.15 g of the adsorbent was added in. The solution pH and adsorption time were kept constant. Fig. 3 demonstrates that the concentration of 10 mg/L is the optimum dye concentration according to the obtained REs. It is obvious that the RE of the adsorption experiments in lower concentrations were approximately as same as the REs in the case of 10 mg/L. Also increasing the dye concentration above 10 mg/L led to the reduction of REs in the performed experiments. This phenomenon is due to the fact that the amount of the adsorbent in the dye removal procedures of the present section is constant where the dye concentration is being increased to observe its consequence in the capability of the adsorbent. So there are only limited sites on the surface of the constant utilized amount of the adsorbent which are occupied by enhancing the dye concentration in the solution. Then extra concentrations of the dye are not adsorbed on the adsorbent due to its saturation. So, 10 mg/L was opted to be utilized in the next experiments.

Investigation of the effect of solution pH

To evaluate the influence of solution pH on REs of the experiments, five dye solution batches containing 10 mg/L

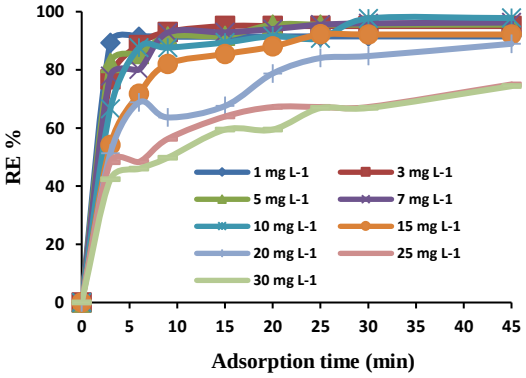

Fig. 3: Effect of the initial concentration of the dye on RE%. Conditions are the same as those used in Fig. 1, except the adsorbent weight was 0.15 g.

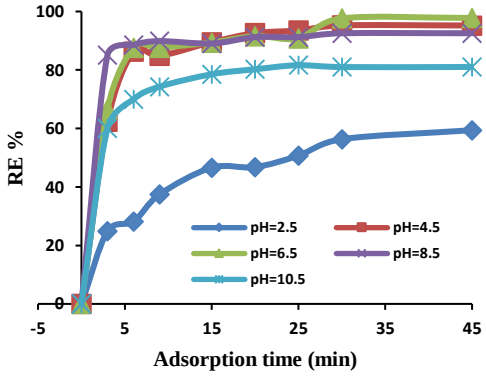

Fig. 4: Effect of the initial pH on RE%. Conditions are the same as those used in Fig. 2, except for the concentration of the dye which was 10 mg/L.

the concentration of crystal violet with different pH levels (2.5, 4.5, 6.5, 8.5, and 10.5) were prepared. The adsorbent weight was kept constant at 0.15 g. Fig. 4 illustrates that the neutral pH is the optimum solution pH for the adsorption process of crystal violet on the utilized adsorbent. As can be seen in the figure, the highly acidic and basic pH values play strictly negative roles in the procedure of pollutant adsorption on the adsorbent. This incident can be attributed to the molecular structure of the adsorbate in acidic and basic pHs which is changed by means of the hydrolysis process that decreases the molecular interactions between the dye and the adsorbent. On the other hand, this can also be because of the alterations in the chemical surface of the adsorbent that dwindles the probability of the generation of intermolecular bonds such as π–π stack and hydrogen bonds. So pH= 6.5 opted as the optimum solution pH in the present survey.

Investigation of the adsorption time

Adsorption time is an influencing parameter in the process of wastewater treatment and the obtained REs. The effect of the adsorption time was investigated during the optimization of adsorbent weight, concentration of dye, and solution pH. The outcome of the experiments illustrated that increasing the adsorption time in different experimental conditions led to the enhancement of REs and after achieving the equilibrium in each case which was found to be around 10 min, and the REs remained constant. The statement is evident by paying attention to Figs. 2, 3, and 4. This event is due to the fact that the dye removal process applied in the present research is based on adsorption, and the adsorption mechanism is a kinetically controlled process that is inherently time-dependent. So reaching a sufficient period of time for the accomplishment of a proper adsorption procedure is of great importance in order to gain high REs in the wastewater treatment process. Accordingly, 10 min opted as the optimum time for the adsorption procedure.

FT-IR characterization

The properties of the studied adsorbent were investigated by FT-IR analysis. The results before and after the adsorption revealed some changes in the obtained spectra. The absorption peaks have been written as cm^{-1} from the FT-IR spectrum of the natural adsorbent before the dye adsorption (Fig. 5a) are related to the bonds in the composition of the adsorbent written in parenthesis: 896.96 (C–H bending), 1156.76 (C–O stretching), 1384.06 (O–H bending), 1516.42 (N–O stretching), 1645.68 (C=C stretching), 2922.14 (C–H stretching), and 3436.86 (O–H stretching). Despite a wide range of overlapping in the FT-IR spectra of (a) and (b) which is due to the complex composition of the natural adsorbent that covers the FT-IR absorption peaks of crystal violet, there are still some absorption peaks at 3442.61 (O–H stretching), 1372.02 (C–H bending), 1171.41 (C–N stretching), 831.95 (C=C bending), and 1123.12 cm^{-1} (C–O stretching) in the structure of the dye (Fig. 5b) which proves the adsorption of crystal violet on the surface of the natural adsorbent. Definitely, the presence of various functional groups in the complicated composition of the adsorbent improves the accomplishment of the adsorption procedure of the dye. For instance, the presence of C=C bond in the adsorbent

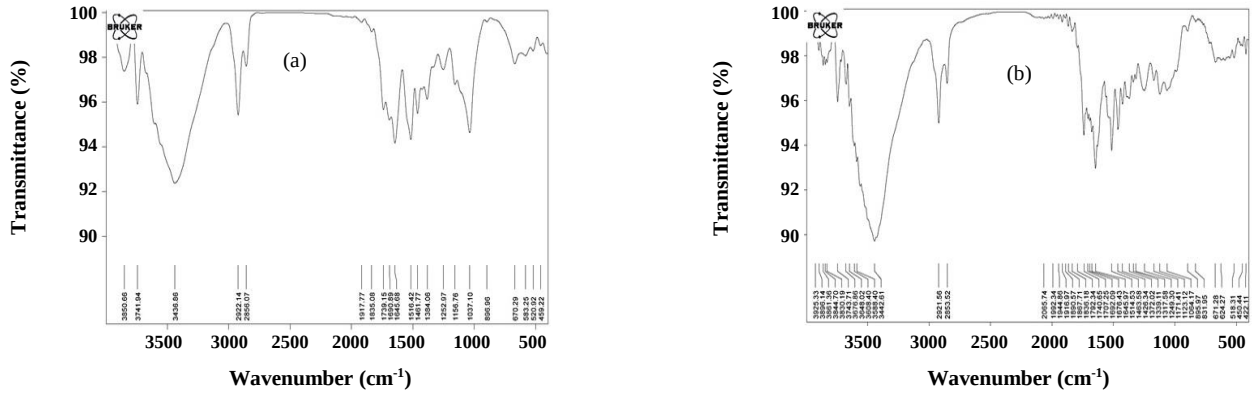

Fig. 5: FT-IR spectra of the adsorbent before (a) and after (b) the adsorption of crystal violet.

the structure which was established by the FT-IR analysis of the adsorbent at 1645.68 cm^{-1}, and also the existence of C=C bonds in the phenyl groups of the dye structure, increase the probability of creating π–π stack interactions which enhances the adsorption efficiency. Moreover, the presence of O–H functional group in the adsorbent composition, and the existence of nitrogen atoms in the amine functional groups of crystal violet amplifies the creation of hydrogen bonds between the adsorbent and the adsorbate which eventually enhances the adsorption of the pollutant on the adsorbent and increases the RE.

The equilibriums of adsorption isotherms

Drawing the linear plots of Langmuir, Freundlich, and Temkin isotherm models demonstrated that the Langmuir isotherm model is the best–fitted isotherm for the adsorption of crystal violet on the surface of the adsorbent with the highest correlation coefficient ($R^2 = 0.979$) among the other surveyed isotherm models. Obedience of the applied adsorbent from Langmuir isotherm model demonstrates that there is a finite number of active sites which are homogeneously distributed over the surface of the adsorbent. These active sites have the same affinity for adsorption of a monomolecular layer and there is no interaction between the adsorbed molecules. So crystal violet dye is a pollutant in the simulated wastewater is adsorbed on the surface of *Populus Alba* homogenously and in a mono-layer mood. The drawn isotherms are illustrated in Fig. 6 (a, b, and c). The obtained parameters of the isotherms are also shown in Table 1.

Adsorption kinetic studies

The kinetic studies of the adsorption procedure were accomplished in different dye concentrations (1, 5, 10, and 20 mg/L) in order to obtain information about the rate of the pollutant adsorption on the adsorbent. Pseudo first order, pseudo-second-order, and Weber–Morris intraparticle diffusion models were analyzed and the obtained linear charts are shown in Figs 7 (a, b, and c). Also, Table 2 demonstrates the obtained constants of the three studied kinetic models. As the results of the kinetic studies show, the correlation coefficients (R^2) of the pseudo-second-order model are greater than the other two studied models. So it can be concluded that the adsorption of the dye on the adsorbent obeys the pseudo-second-order kinetic model.

ANN modeling

As previously mentioned, 10 nodes were utilized in the hidden layer for the accomplishment of the ANN procedure. For the investigation of the nodes numbers in the modeling, a series of nodes from 2 to 20 (with the intervals of two nodes) were chosen and each topology was repeated three times. Eq. 8 was used to calculate the mean square error.

$$MSE = \frac{1}{Q}\sum_{i=1}^{i=Q}\left(y_{i,pred} - y_{i,exp}\right)^2 \quad (8)$$

In the above–mentioned equation, i is an index of data, Q is the number of data points, $y_{i,exp}$ expresses the experimental response, and $y_{i,pred}$ illustrates the network prediction. The relation between the neurons number in the hidden layer and network error is illustrated in Fig. 8. Obviously, MSE is minimum when there are 10 neurons. The developed ANN model was applied for the comparison of the experimental and calculated data for validation, training, test, and all data set which is shown in Fig. 9. The correlation coefficients of the training,

Table 1: Isotherm parameters for adsorption of the dye on the adsorbent.

Isotherm model	Parameter	Quantity
Langmuir	q_{max} B R^2	12.25 1.04 0.979
Freundlich	K_f n R^2	4.74 2.10 0.790
Temkin	B K R^2	2.17 1.53 0.934

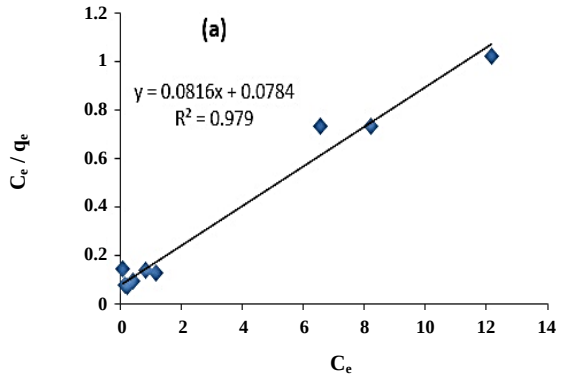

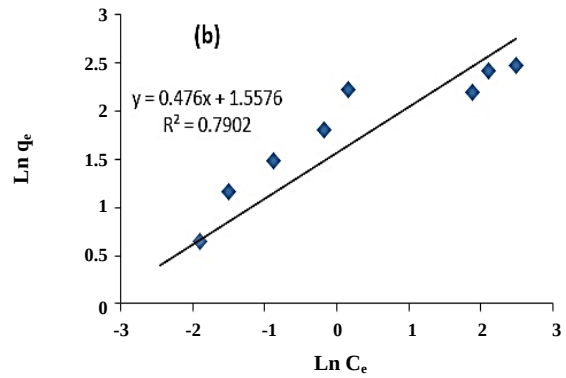

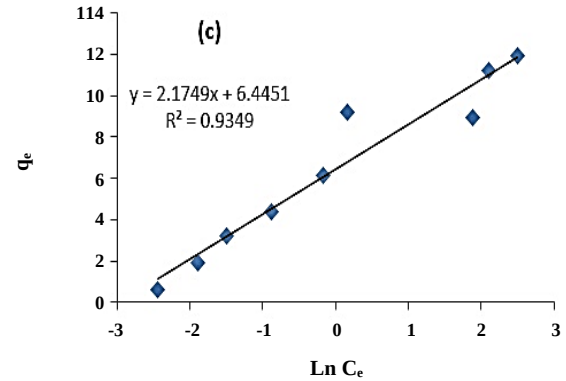

Fig. 6: Fit of (a) Langmuir, (b) Freundlich, and (c) Temkin isotherm models for the adsorption of crystal violet on the adsorbent.

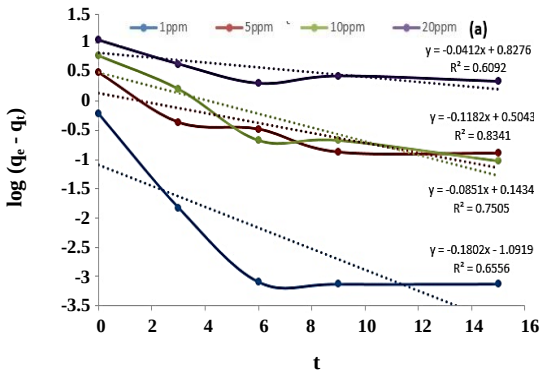

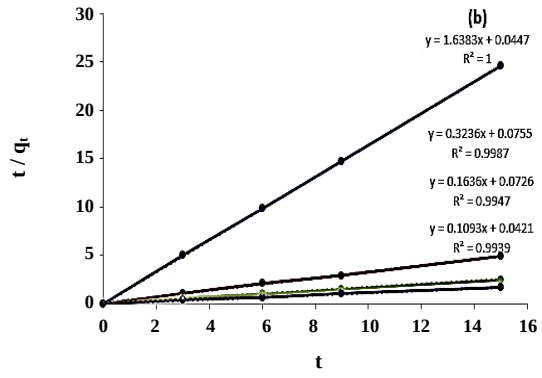

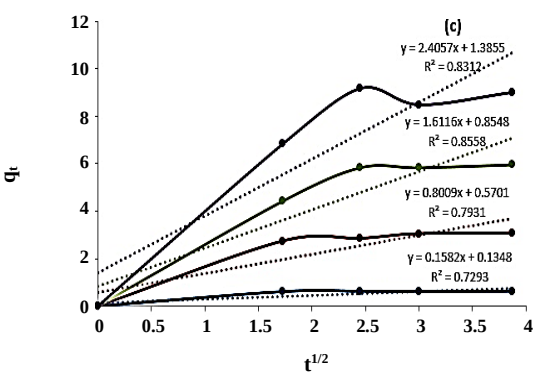

Fig. 7: Fit of (a) pseudo first, (b) second order, and (c) Weber–Morris intra–particle diffusion kinetic models for the adsorption of crystal violet on the adsorbent.

Table 2: Values of the kinetic study for the adsorption of the dye on the adsorbent.

	Weber–Morris intra–particle diffusion			Pseudo first order			Pseudo second order		
Concentration (mg/L)	k_i (mg g^{-1} $min^{-1/2}$)	c (mg/g)	R^2	q_e (mg/g)	k_1 (min^{-1})	R^2	q_e (mg/g)	k_2 (g mg^{-1} min^{-1})	R^2
1	0.158	0.135	0.729	0.081	0.414	0.656	0.611	59.525	1.000
5	0.801	0.570	0.793	1.389	0.196	0.750	3.086	1.408	0.998
10	1.612	0.855	0.856	3.192	0.272	0.834	6.097	0.368	0.994
20	2.406	1.385	0.831	6.729	0.094	0.609	9.174	0.283	0.993

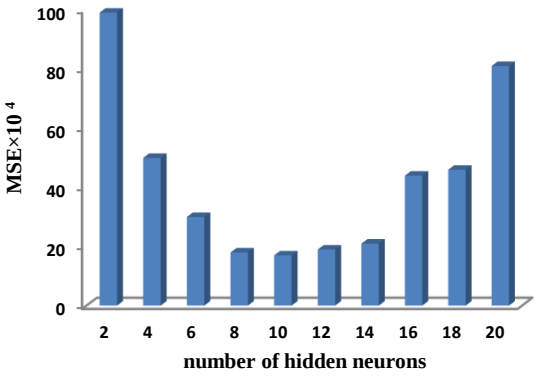

Fig. 8: Consequence of the number of applied neurons in the hidden layer of the model on the performance of the network.

validation and test series were achieved to be 0.988, 0.988, and 0.961, respectively. The overall correlation coefficient of the modeling was also found to be 0.980 which illustrates the appropriate modeling of the system. This means that the prediction of the results of the experiment becomes possible by using the currently developed model. Moreover, upscaling the treatment process for industrial applications is possible by learning from the developed ANN model. The total outcome of the ANN process proves the successful modeling of the environmental–friendly adsorption procedure due to having a considerable match between the experimental and predicted data.

Comparison of the applied adsorbent with other adsorbents

In order to have comprehensive information among the studied natural adsorbents for the aim of pollutant removal from wastewater media, some features of the applied procedures such as the adsorbent, removed pollutant, the isotherm, kinetic, and ANN models and their correlation coefficients and q_{max} values were investigated and compared with the applied adsorbent in the present survey. The outcome of the comparison shown in Table 3 illustrates that, unlike some other surveys, this investigation comprises isotherm, kinetic, and ANN modeling which makes it a comprehensive study. As like as most of the mentioned surveys, this study also obeys the Langmuir isotherm and pseudo-second-order kinetic models which illustrates monolayer chemisorption procedures in such adsorbents. Acceptable q_{max} value and comparable correlation coefficients of the isotherm and ANN models demonstrate the efficiency of the applied adsorbent in the process of wastewater treatment.

CONCLUSIONS

The present research demonstrates the adsorptive ability of the sawdust of *Populus alba* trees' pruned hardwood as an agricultural waste material that is capable and highly recommended to be used in wastewater treatment procedures. Moreover to the usage of this waste pruned material in the wastewater refinery process, this procedure is supposed to be a helpful waste management progression and also the residue of the adsorbent after the accomplishment of the treatment procedure can be utilized for the production of particleboards with veneer. The adsorbent showed its optimum adsorptive capability in neutral pH (pH= 6.5), so there is no need for pH variation which makes it so economical for further industrial usage. The optimum weight of adsorbent and dye concentration were found to be 0.15g and 10 mg/L, respectively. Also increasing the REs were observed by decreasing the initial dye concentration and increasing the weight of adsorbent. Moreover, increasing the adsorption time to 10 min heightened the REs of the fulfilled treatment experiments. The obtained data from the isotherm studies demonstrated that the adsorption process was best fitted by the Langmuir isotherm model with the highest correlation coefficient of

Table 3: Comparison of the applied adsorbent with other adsorbents.

Adsorbent	Removed pollutant	Isotherm model	Kinetic model	Isotherm R^2	ANN R^2	q_{max} (mg g^{-1})	Ref.
Soya bean waste	Methyl violet 2B	Langmuir	Pseudo second order	0.997	0.994	180.7	[50]
Activated carbon of rattan sawdust	Methylene blue	Langmuir	Pseudo second order	0.999	–	294.14	[51]
Parthenium biomass	Rhodamine-B	Langmuir	Pseudo second order	0.971	–	28.82	[52]
Do Ghazal tea waste	Malachite Green	Freundlich	–	0.993	0.998	–	[19]
Pretreated Sesamum indicum seeds' waste	Diethyl phthalate, Butylated hydroxy anisole, Butylated hydroxy toluene	Langmuir (for all pollutants)	–	0.982, 0.992, 0.995	0.994	0.226, 0.292, 0.128	[35]
Iranian golden Sesamum indicum hull	Acid red 88	Langmuir	–	0.984	–	25	[9]
Populus Alba	Crystal violet	Langmuir	Pseudo second order	0.979	0.98	12.25	Present work

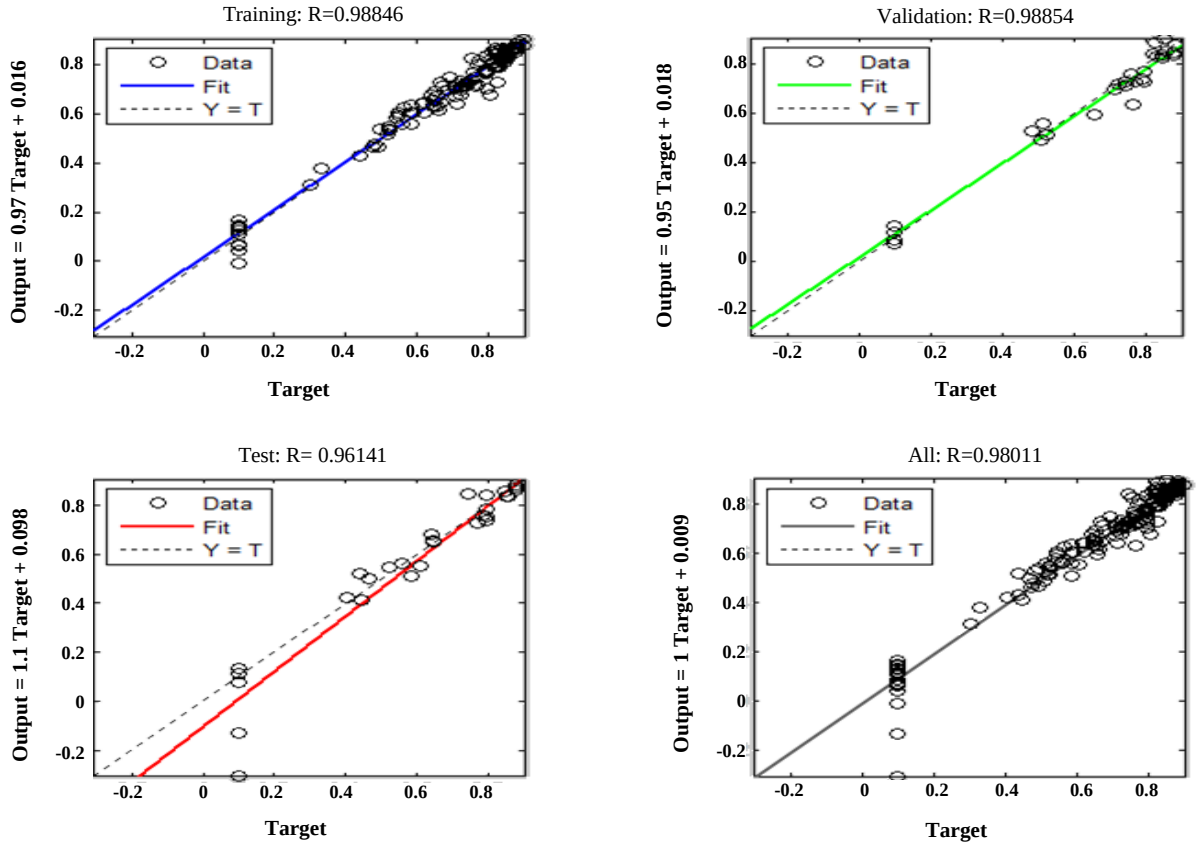

Fig. 9: Comparison of the predicted data via the applied ANN model with the obtained experimental data for the training, validation, test, and all data series.

R^2 = 0.979 among the other studied isotherm models. The q_{max} value obtained from the Langmuir isotherm was also calculated to be 12.25 mg/g. Also, the kinetic survey illustrated that the adsorption of the dye on the adsorbent obeys the pseudo-second-order kinetic model. The results of the ANN model containing three–layer of input variables, a hidden layer, and an output section vividly proved the fitness of theoretical and experimental data according to the obtained correlation coefficient values which were more than 0.96.

Received : May. 13, 2020 ; Accepted : July 6, 2020

REFERENCES

[1] Javad A.H., Al–Heetim D.T.A., Mastuli M.S., Biochar from Orange (Citrus Sinensis) Peels by Acid Activation for Methylene Blue Adsorption, *Iran. J. Chem. Chem. Eng. (IJCCE)*, **38(2)**: 91–105 (2019).

[2] Shahsavani S., Dehghani M., Shamsedini N., Removal of Direct Red 81 from Aqueous Solution Using an Acidic Soil Containing Iron (Case Study of Lahijan Soil), *Iran. J. Chem. Chem. Eng. (IJCCE)*, **38(2)**: 107–112 (2019).

[3] Zollinger H., "Color Chemistry: Syntheses, Properties and Applications of Organic Dyes and Pigments", VCH Publishers, New–York, (1987).

[4] Al–Degs Y.S., El–Barghouthi M.I., El–Sheikh A.H., Walker G.M., Effect of Solution pH, Ionic Strength, and Temperature on Adsorption Behavior of Reactive Dyes on Activated Carbon, *Dyes Pigments*, **77**: 16–23 (2008).

[5] McKay G., Otter burn M.S., Sweeney A.G., The Removal of Color from Effluent Using Various Adsorbents Silica: Rate Process, *Water Res*., **14(1)**: 15–20 (1980).

[6] Rosenkranz H.S., Cunningham S.L., Mermelstein R., Cunningham A.R., The Challenge of Testing Chemicals for Potential Carcinogenicity Using Multiple Short–Term Assays: An Analysis of a Proposed Test Battery for Hair Dyes, *Mutat. Res–Gen Tox. En*., **633**: 55–66 (2007).

[7] Kayan B., Gözmen B., Demirel M., Gizir A.M., Degradation of Acid Red 97 Dye in Aqueous Medium Using Wet Oxidation and Electro–Fenton Techniques, *J. Hazard. Mater*., **177**: 95–102 (2010).

[8] Bayram E., Ayranci E., Electrochemically Enhanced Removal of Polycyclic Aromatic Basic Dyes from Dilute Aqueous Solutions by Active Carbon Cloth Electrodes, *Environ. Sci. Technol*., **44 (16)**: 6331–6336 (2010).

[9] Zarei M., Pezhhanfar S., Ahmadi Someh A., Removal of Acid Red 88 from Waste Water by Adsorption on Agro-Based Waste Material. A Case Study of Iranian Golden Sesamum indicum Hull, *Environ. Health. Eng. Manag. J.*, **4(4)**: 195–201 (2017).

[10] Mahmoodabadi M., Khoshdast H., Shojaei V., Efficient Dye Removal from Aqueous Solutions Using Rhamnolipid Biosurfactants by Foam Flotation, *Iran. J. Chem. Chem. Eng. (IJCCE)*, **38(4)**: 127–140 (2019).

[11] Tan B.H., Teng T.T., Omar A.K.M., Removal of Dyes and Industrial Dye Wastes by Magnesium Chloride, *Water Res*., **34**:597–601 (2000).

[12] LaPara T.M., Konopka A., Nakatsu C.H., Alleman J.E., Thermophilic Aerobic Wastewater Treatment in Continuous–Flow Bioreactors, *J. Environ. Eng*., **126**:739–744 (2000).

[13] Bell J., Plumb J.J., Buckley C.A., Stuckey D.C., Treatment and Decolorization of Dyes in an Anaerobic Baffled Reactor, *J. Environ. Eng*., **126**: 1026–1032 (2000).

[14] Zouboulis A.I., Lazaridis N.K., Grohmann A., Toxic Metals Removal from Waste Waters by up Flow Filtration with Floating Filter Medium. I. The Case of Zinc, *Sep. Sci. Technol*., **37**: 403–416 (2002).

[15] Bolto B., Dixon D., Eldridge R., King S., Linge K., Removal of Natural Organic Matter by Ion Exchange, *Water Res*., **36**:5057–5065 (2002).

[16] Lin S.H., Juang R.S., Removal of Free and Chelated Cu (II) Ions from Water by a Nondispersive Solvent Extraction Process, *Water Res*., **36**: 3611–3619 (2002).

[17] Esplugas S., Gimenez J., Contreras S., Pascual E., Rodriguez M., Comparison of Different Advanced Oxidation Processes for Phenol Degradation, *Water Res.*, **36**: 1034–1042 (2002).

[18] Shen H., Wang Y.T., Biological Reduction of Chromium by *E. Coli*. *J. Environ. Eng*., **120**: 560–571 (1994).

[19] Zarei M., Fazli S., Najjari N., Pezhhanfar S., Ahmadi Someh A., Efficiency of Artificial Neural Networks for Modeling of Malachite Green Adsorption by Tea Waste and Adsorption Isotherm Study, *J. Water Wastewater*, **30(6)**: 51–62 (2019).

[20] Szpyrkowicz L., Naumczyk J., Zilio–Grandi F., Electrochemical Treatment of Tannery Wastewater Using Ti/Pt and Ti/Pt/Ir Electrodes, *Water Res*., **29**:517–524 (1995).

[21] Khelifi O., Nacef M., Affoune A.M., Nickel (II) Adsorption from Aqueous Solutions by Physico–chemically Modified Sewage Sludge, *Iran. J. Chem. Chem. Eng. (IJCCE)*, **37(1)**: 73–87 (2018).

[22] Robinson T., Chandran B., Nigam P., Studies on Desorption of Individual Textile Dyes and a Synthetic Dye Effluent from Dye–adsorbed Agricultural Residues Using Solvents, *Bioresour. Technol*., **84(3)**: 299–301 (2002).

[23] Pavan F.A., Gushikem Y., Mazzocato A.S., Dias S.L.P., Lima E.C., Statistical Design of Experiments as a Tool for Optimizing the Batch Conditions to Methylene Blue Biosorption on Yellow Passion Fruit and Mandarin Peels, *Dyes Pigments*, **72**: 256–266 (2007).

[24] Aksu Z., Kabasakal E., Batch Adsorption of 2,4–Dichlorophenoxy–acetic acid (2,4–*D*) from Aqueous Solution by Granular Activated Carbon, *Sep. Purif. Technol*., **35**: 223–240 (2004).

[25] Attia A.A., Girgis B.S., Fathy N.A., Removal of Methylene Blue by Carbons Derived from Peach Stones by H_3PO_4 Activation: Batch and Column Studies, *Dyes Pigments*, **76**: 282–289 (2008).

[26] Garg V.K., Gupta R., Juneja T., Removal of a Basic Dye (Rhodamine–B) from Aqueous Solution by Adsorption Using Timber Industry Waste, *Chem. Biochem. Eng. Q*, **18(4)**: 417–22 (2004).

[27] Sivarajasekar N., Baskar R., Optimization, Equilibrium and Kinetic Studies of Basic Red 2 Removal onto Waste Gossypium hirsutum Seeds, *Iran. J. Chem. Chem. Eng. (IJCCE)*, **37(2)**: 157–169 (2018).

[28] Ba S., Karima E., Abdelrani Y., Abdelhakim A., Abdelaziz B., Activated Carbon from Olive Wastes as an Adsorbent for Chromium Ions Removal, *Iran. J. Chem. Chem. Eng. (IJCCE)*, **37(6)**: 107–123 (2018).

[29] Asfour H.M., Nassar M.M., Fadali O.A., EL–Geundi M.S., Color Removal from Textile Effluents Using Hardwood Sawdust as an Absorbent, *J. Chem. Technol. Biotechnol*., **35(1)**: 28–35 (1985).

[30] Gong R., Sun Y., Chen J., Liu H., Yang C., Effect of Chemical Modification on Dye Adsorption Capacity of Peanut Hull, *Dyes Pigments*, **67**: 175–181 (2005).

[31] Garg V.K., Moirangthem A., Rakesh K., Renuka G., Basic Dye (Methylene Blue) Removal from Simulated Wastewater by Adsorption Using Indian Rosewood Sawdust: a Timber Industry Waste, *Dyes Pigments*, **63(3)**: 243–250 (2004).

[32] Lata H., Garg V.K., Gupta R.K., Removal of a Basic Dye from Aqueous Solution by Adsorption Using Parthenium Hysterophorus: An Agricultural Waste, *Dyes Pigments*, **74**: 653–658 (2007).

[33] Tunc O., Tanacı H., Aksu Z., Potential Use of Cotton Plant Wastes for the Removal of Remazol Black B Reactive Dye, *J. Hazard. Mater*., **163**: 187–198 (2009).

[34] Namasivayam C., Muniasamy N., Gayatri k., Rani M., Ranganathan K., Removal of Dyes from Aqueous Solutions by Cellulosic Waste Orange Peel, *Bioresour. Technol*., **57(1)**: 37–43 (1996).

[35] Farajzadeh M.A., Pezhhanfar S., Zarei M., Mohebbi A., Simultaneous Elimination of Diethyl Phthalate, Butylated Hydroxy Toluene and Butylated Hydroxy Anisole from Aqueous Medium by an Adsorption Process on Pretreated Waste Material; Investigation of Isotherms and Neural Network Modeling, *J. Iran. Chem. Soc*., **17**: 1377–1386 (2020).

[36] https://en.wikipedia.org/wiki/Populus_alba. (Accessed 10 February 2020).

[37] Kinniburgh D.G., General Purpose Adsorption Isotherms, *Environ. Sci. Technol*., **20(9)**: 895–904 (1986).

[38] Vijayakumar G., Tamilarasan R., Dharmendirakumar M., Adsorption, Kinetic, Equilibrium and Thermodynamic Studies on the Removal of Basic Dye Rhodamine-B from Aqueous Solution by the Use of Natural Adsorbent Perlite, *J. Mater. Environ. Sci.*, **3(1)**: 157–170 (2012).

[39] Girisuta B., Danon B., Manurung R., Janssen L., Heeres H., Experimental and Kinetic Modelling Studies on the Acid–Catalysed Hydrolysis of the Water Hyacinth Plant to Levulinic Acid, *Bioresour. Technol. Rep*., **99(17)**:8367–8375 (2008).

[40] Theydan S.K., Ahmed M.J., Adsorption of Methylene Blue onto Biomass-Based Activated Carbon by FeCl3 Activation: Equilibrium, Kinetics, and Thermodynamic Studies, *J. Anal. Appl. Pyrolysis*., **97**: 116–122 (2012).

[41] Tunc O., Tanacı H., Aksu A., Potential Use of Cotton Plant Wastes for the Removal of Remazol Black B Reactive Dye, *J. Hazard. Mater.*, **163**: 187–198 (2009).

[42] Kumar A., Kumar S., Kumar S., Adsorption of Resorcinol and Catechol on Granular Activated Carbon: Equilibrium and Kinetics, *Carbon*, **41**: 3015–3025 (2003).

[43] Lorenc–Grabowska E., Gryglewicz G., Adsorption Characteristics of Congo Red on Coal-Based Mesoporous Activated Carbon, *Dyes pigments*, **74**: 34–40 (2007).

[44] Chowdhury S., Das Saha P., Artificial Neural Network (ANN) Modeling of Adsorption of Methylene Blue by NaOH-Modified Rice Husk in a Fixed-bed Column System, *Environ. Sci. Pollut. Res*., **20**: 1050–1058 (2013).

[45] Guiné R.P.F., Gonçalves C., Matos S., Gonçalves F., Costa D.V.T.A., Mendes M., Modeling Through Artificial Neural Networks of the Phenolic Compounds and Antioxidant Activity of Blueberries, *Iran. J. Chem. Chem. Eng. (IJCCE)*, **37(2)**: 193–212 (2018).

[46] Devani M., Oubagaranadin J.U.K., Munshi B., Lal B.B., Mandal S., BP-ANN Approach for Modeling Cd(II) Bio-Sorption from Aqueous Solutions Using Cajanus cajan Husk, *Iran. J. Chem. Chem. Eng. (IJCCE)*, **38(1)**: 111–125 (2019).

[47] Samadani E., Shamekhi, A.H., Behroozi M.H., Chini R., A Method for Pre-Calibration of DI Diesel Engine Emissions and Performance Using Neural Network and Multi-Objective Genetic Algorithm, *Iran. J. Chem. Chem. Eng. (IJCCE)*, **28(4)**: 61–70 (2009).

[48] Tumer A.E., Edebali S., Gulcu S., Modeling of Removal of Chromium (VI) from Aqueous Solutions Using Artificial Neural Network, *Iran. J. Chem. Chem. Eng. (IJCCE)*, **39(1)**: 163–175 (2020).

[49] Zahedi Abghari S., Imani A., Determination of Suitable Operating Conditions of Fluid Catalytic Cracking Process by Application of Artificial Neural Network and Firefly Algorithm, *Iran. J. Chem. Chem. Eng. (IJCCE)*, **37(6)**: 157–168 (2018).

[50] Rahimi Kooh M.R., Dahri M.K., Lim L.B.L., Lim L.H., Malik O.A., Batch Adsorption Studies of the Removal of Methyl Violet 2B by Soya Bean Waste: Isotherm, Kinetics and Artificial Neural Network Modelling, *Environ. Earth Sci*., **75**:783–797(2016).

[51] Hameed B.H., Ahmad A.L., Latiff K.N.A., Adsorption of Basic Dye (Methylene Blue) onto Activated Carbon Prepared from Rattan Sawdust, *Dyes pigments*, **75**: 143–149 (2007).

[52] Lata H., Mor S., Garg V.K., Gupta R.K., Removal of a Dye from Simulated Wastewater by Adsorption Using Treated Parthenium Biomass, *J. Hazard. Mater*., **153**: 213–220 (2008).